Nuevo modelo canónico de seguidor solar para ensayo en túnel aerodinámico

Introduction of a new benchmark for single-axis solar trackers: standardizing wind tunnel testing and comparative analysis

Carlos Rodríguez-Casado[a], José Luis Ruiz-Moral[b], Juan Andrés Cárdenas-Rondón[c], Eduardo Blanco-Marigorta[d], Sebastián Franchini Longhi[e], Antonio Navarro-Manso[f]

[a] MSc Civil Engineer. University of Oviedo, Energy. PhD Candidate FPU. rodriguezccarlos@uniovi.es

[b] Aeronautical Engineer. Polytechnic University of Madrid, IDR. PhD Candidate FPU. joseluis_ruizmoral@hotmail.com

[c] PhD Aeronautical Engineer. Polytechnic University of Madrid, IDR. Associate Professor. ja.cardenas@upm.es

[d] PhD Industrial Engineer. University of Oviedo, Energy. Full Professor. eblanco@uniovi.es

[e] PhD Aeronautical Engineer. Polytechnic University of Madrid, IDR. Full Professor. s.franchini@upm.es

[f] PhD Civil Engineer. University of Oviedo, Energy. Professor. navarroantonio@uniovi.es

RESUMEN

Este estudio propone un nuevo modelo a escala para ser utilizado como referencia en el ensayo aeroelástico en túnel aerodinámico de seguidores solares fotovoltaicos de un solo eje. Ha sido diseñado y construido replicando meticulosamente las características geométricas y elasto-mecánicas de un prototipo representativo del mercado actual. Este modelo canónico permite el análisis comparado y revisado por pares de la inestabilidad torsional que experimentan estas estructuras bajo la acción del viento, fomentando así la colaboración y el intercambio de conocimiento entre centros de investigación y constructores, así como la redacción de códigos específicos sobre la interacción fluido-estructura.

ABSTRACT

This study proposes a novel scale model to serve as a reference for aeroelastic wind tunnel testing of single-axis photovoltaic solar trackers. The model has been meticulously designed and constructed, with precise replication of the geometrical and elastic-mechanical characteristics of a real-world prototype. This model enables a comparative and peer-reviewed analysis of the torsional instability experienced by these structures under the action of wind, thereby fostering collaboration, knowledge exchange between research centers and builders, and the drafting of regulatory codes that specifically address fluid-structure interaction.

PALABRAS CLAVE: modelo, túnel aerodinámico, aeroelasticidad, inestabilidad torsional.
KEYWORDS: scale model, wind tunnel, aeroelasticity, torsional instabilities.

1. Introduction

This communication introduces a novel benchmark for single-axis solar trackers, emphasizing the geometric and construction aspects essential for wind tunnel testing. The benchmark, derived from real-world prototypes, accurately replicates aeroelastic phenomena such as torsional instabilities critical for structural integrity and energy efficiency. By providing a standardized framework [1], this benchmark facilitates comparative analysis among wind tunnel laboratories, enabling advancements in single-axis solar tracker knowledge, design and performance [2].

The utilization of single-axis solar trackers (*SAT*) in renewable energy systems has exhibited an upward trend, consequently, a comprehensive understanding of their dynamic behavior under wind loading is crucial [3].

A substantial research endeavor is currently underway to investigate the aeroelastic behavior of *SAT* under wind loading. However, the range of geometric and physical configurations of engineering interest is extensive [4]. Furthermore, the associated fluid-structure interaction phenomena [5] are intricate, to the extent that there exist multiple potential excitation mechanisms that can lead to instability, which can concurrently affect each other. Researchers [6] have defined the primary aeroelastic mechanisms involved in torsional instability and have compared the results using various methods.

Available data from tests and simulations are limited and dispersed, and our current knowledge of the fundamental phenomena related to *SAT* aeroelasticity can still be considered limited [7]. There is an increasing need to establish a set of criteria and test conditions [6, 8] that are suitable for investigating the aeroelastic response of a reference *SAT*. This would allow for the adequate reproduction and contrast of measurement data and predictions from simulations [9].

The proposed benchmark meticulously replicates the geometric and construction features of real single-axis solar trackers, ensuring scalability from prototype to testing model. Similarity laws must be matched and all the elements, especially the hinges, the fixed section, the inertia, and stiffness of the torque tube has been reproduced. And by measuring forces on the driver and deflections all along the tracker, the one single degrre of freedom (*1DOF)* flutter or "*galloping*" is thoroughly characterized.

Two complete series of tests have been conducted in two different wind tunnles (*ACLA16* at Polytechnic School of Madrid IDR and *ETHAN50-ablWT* at University of Oviedo EPM), with two copies of the benchmark. The agreement of the results is really good, validating the proposed model.

2. Design of the benchmark

A single-axis solar tracker is a structure consisting of multiple photovoltaic panels mounted on a horizontal axis, known as a torque tube. A motor (usually in the middle of the two wings) rotates the tracker, thereby allowing the angle of inclination of the panels to vary progressively each day, from east to west, with the objective of maximizing the amount of solar energy captured by the cells (Figure 1).

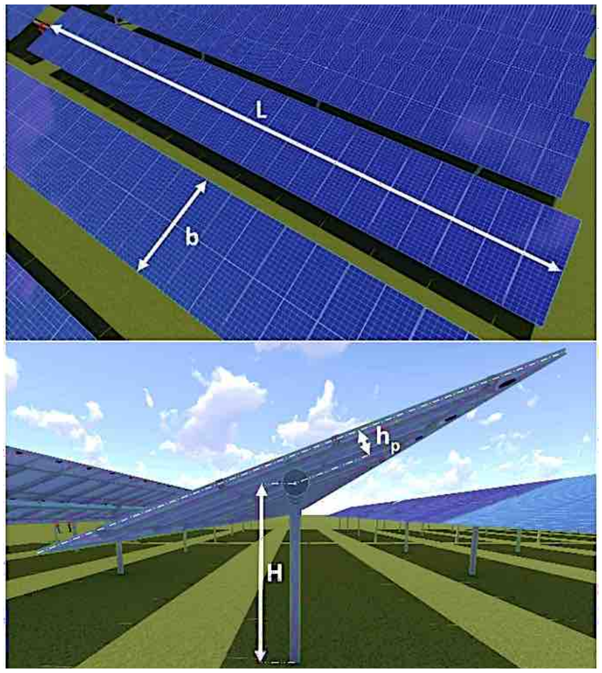

Figure 1. Render of the prototype of *SAT*.

Structurally, this system possesses a degree of freedom corresponding to torsional rotation, as the supports distributed along the tube effectively prevent any significant displacement in the radial direction. In such systems, the first mode of vibration is typically a low-frequency helical torsion (of the order of 1 Hz), which does not generate any deflection on the motor shaft but causes opposite rotation at both ends.

The pursuit of cost reduction in such a competitive industrial sector has given rise to the adoption of narrower torque tube designs, which, when coupled with large flat plates that may be exposed to wind load, frequently result in *SAT* manifesting aerodynamic instability including torsional galloping or single-degree-of-freedom flutter, vortex-induced vibration, and buffeting.

2.1 Prototype

The prototype has been elected with two independent vertical rows of panels (*2P*), consisting of 96 panels (48 each wing). The solar panels have been taken to be 2.4 m long and 1.2 m wide, one of the biggest among all the possibilities in the industry.

The total length of the tracker is 2 L_p = 57.60 m (L_p = 28.80 m), and the chord is b_p = 4.80 m. The aspect ratio ($AR=2L/b$) is 12, which is representative of the systems with 2 modules-in-portrait (*2P*). The systems with one module-in-portrait (*1P*) usually have a larger aspect ratio. However, this benchmark also represents a “short” 1P tracker at double scale.

Figure 2 shows all the structural elements of a *SAT*. The torque tube is made of steel with a circular cross section of diameter D_p = 200 mm and thickness e_p = 4 mm. It is supported by 6 pillars (3 per wing). The distance from the tube axis to the ground (height) is H_p = 3 m, and the distance to the panels (clearance) is h_p = 0.24 m. In the variables, subscripts *p* and *m* are used to refer to the prototype and model respectively.

The panels are attached to the torque tube with rectangular steel purlins of 80x40 mm section and 2 mm thick. The purlins are as long as the tracker's width (larger than the newest trend), with 49 purlins per wing. The nominal mass of the panels is 15 kg/m^2, with an additional 25% weight considered for purlins and fastenings.

With regard to the natural frequencies of the prototype, the primary frequency is that of the torsional mode, as previously indicated. It is governed by the torsional stiffness and the rotational inertia. The torsional stiffness is essentially that of the torque tube, as the contribution of the panels is negligible. However, the inertia of this movement is predominantly attributable to the mass of the panels and purlins.

Figure 2. Structural elements of a SAT: torque tube, panels, purlins, pillars and driver.

The torsional stiffness, for a fixed-free tube with a moment at the free end, is calculated in Eq. (1), where *G* is the shear modulus (80.80 GPa for steel), and *J* is the polar moment of inertia of the torque tube.

$$K_{Tp} = \frac{GJ}{L} = 6.64 \cdot 10^4 \text{ N} \cdot \text{m} \quad (1)$$

The rotational inertia of the tracker (Mass Moment of Inertia with respect to the torsional axis) considering panels, purlins, and tube, is I_{Rp} = 5.14·10^3 kg·m^2.

The prototype's natural torsional frequency can be calculated using the following expression:

$$f_{Tp} = \frac{1}{4}\sqrt{\frac{GJ}{I_{Rp}L}} = \frac{1}{4}\sqrt{\frac{K_{Tp}}{I_{Rp}}} = 0.90 \text{ Hz} \quad (2)$$

A finite element study (*FEM*) was conducted to determine the series and frequencies of higher vibration modes. Since the bending movement of the panels overlaps with the torsional movement, its flexural vibration has also been studied, considering the resultant mass and stiffness. The total mass of a wing is M_p = 2592 kg. The flexural stiffness is a function of EI, where E is the Young's modulus, and I is the second moment of area. It has been calculated that the composite value (steel for the purlins and glass for the cells) is approximately $(EI)_p = 2.30 \cdot 10^5$ N·m².

The consideration of alternative vibration modes for this prototype has not been incorporated. However, the prevailing trend of employing shorter purlins with reduced dimensions and panels with more slender frames has the potential to induce plate vibration frequencies. Furthermore, depending on their height and section, pillars could also generate modes that interfere with the phenomenon.

2.2 Similarity laws

In the context of the torsional aeroelastic instability of *SAT*, the variables that must be considered include the characteristic length (L) typically the span or chord, plus to the fluid variables of velocity (U), density (ϱ) and viscosity (μ). In addition to these, structural effects must be taken into account, including torsional stiffness (K_T) and rotational inertia relative to the tube axis (I_R) in the case of torsion of the torque tube, and mass (m) and bending stiffness (EI) in the case of bending of the panels. Furthermore, structural damping (ζ) should be considered.

The variable corresponding to the results would be the torque (T) or, in the event of vibration, the moment amplitude and frequency (f_M) of the resulting aeroelastic excitation. It should be noted that gravity exerts no influence due to the obstruction of vertical movements by the pillars.

In order for the experimental results to be applicable to the prototype, it is necessary to ensure that the dimensionless numbers of the phenomena in the wind tunnel and in reality are equal, i.e.:

$$Re = \frac{\rho U L}{\mu} \tag{3}$$

is the Reynolds (Re) number from the variables of the fluid.

$$C_{KT} = \frac{GJ}{\rho U^2 L^4} = \frac{K_T}{\rho U^2 L^3} \tag{4}$$

$$C_{IR} = \frac{I_R}{\rho L^5} \tag{5}$$

$$C_{KF} = \frac{EI}{\rho U^2 L^4} \tag{6}$$

$$C_M = \frac{M}{\rho L^3} \tag{7}$$

are respectively the torsional stiffness, the rotational inertia, the flexural stiffness and the mass coefficients, from the structural variables, plus the damping which is already dimensionless.

$$C_T = \frac{T}{\frac{1}{2}\rho U^2 b^2 L} \tag{8}$$

$$St = \frac{fL}{U} \tag{9}$$

are the numbers related to the results, the Euler number (Eu) or torque coefficient and the Strouhal number (St).

Finally, it is noteworthy that unlike the other variables requiring similarity transformations, the angles are the same in model and prototype, under similarity conditions.

2.3 Scale model

The specifications of the aeroelastic model have been defined for a half tracker due to the symmetry with respect to the driver. A scale ratio of $\lambda = 1/30$ has been chosen, the model length is L_m = 960 mm, the chord b_m = 160 mm, and the height of the axis above the ground H_m = 100 mm. The panels and supports have been manufactured using 3D printing with *PLA*

(*Polylactic Acid*), and a brass tube has been used for the torque tube, although aluminum and carbon fiber tubes have been also built and tested.

2.3.1. Panels

In order to facilitate the manufacturing process, the panels have been arranged into groups of four (*2V2H*), thus yielding a total of 12 groups per wing (Figure 3a). A small gap has been maintained between them when mounted on the torque tube, and it has been determined that this configuration does not modify the torsional stiffness of the model. The panels are constant thickness, 0.4 mm, positioned at a distance h_m = 8 mm to the axis. The are three longitudinal purlins, with the aim of ensuring that the bending stiffness of the plates in the direction of the chord is equivalent to that of the prototype. They have a depth of 4 mm and a width of 0.80 mm. Brackets have been designed to attach the panels to the tube (Figure 3b), using epoxy resin.

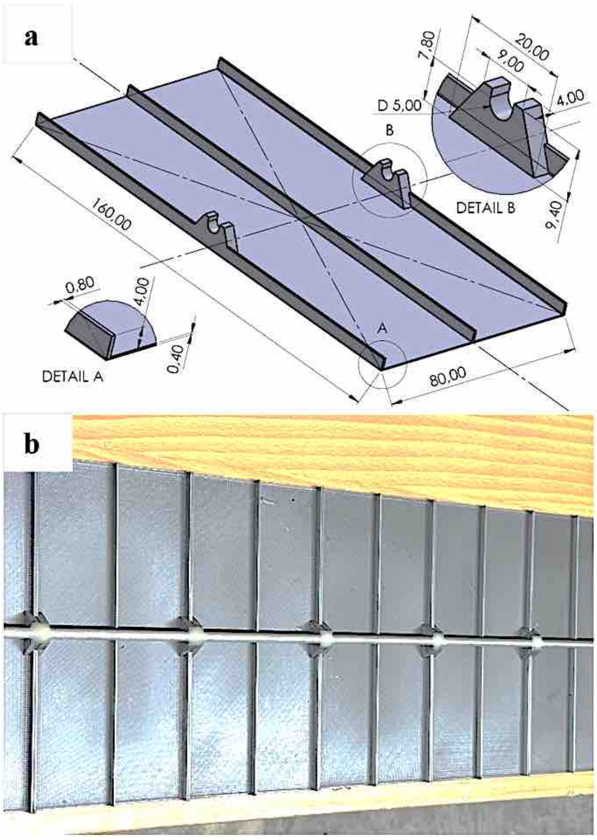

Figure 3. Scale model panels: a) technical drawing; b) assembly on aluminum torque tube.

From the identity of C_{IR} coefficient:

$$\frac{I_{Rm}}{I_{Rp}} = \left(\frac{L_m}{L_p}\right)^5 \tag{10}$$

I_{Rm}=2.17·10^{-4} kg·m^2. This value differs only by 3% from the due ratio.

2.3.2. Torque tube

A 1-meter-long brass tube (*EN-CW507L*) has been used to attach the model to the driver fixed end. The outer diameter of the tube is D_m = 5 mm, with a wall thickness of e_m = 0.50 mm. According to the scale, the diameter should be 6.6 mm, but a slightly smaller tube has been chosen to reduce the necessary air velocities in the wind tunnel. It has been found that the tube diameter does not significantly influence the phenomenon.

With a shear modulus for brass of G = 40 GPa, the model's torsional stiffness is K_{Tm} = 1.51 N·m. The relationship between the stiffnesses of the model and prototype is an equation with one degree of freedom:

$$\frac{K_{Tm}}{K_{Tp}} = \left(\frac{U_m}{U_p}\right)^2 \left(\frac{L_m}{L_p}\right)^3 \tag{11}$$

By choosing the torsional stiffness, the relationship between the real speed and the wind tunnel speed is fixed:

$$\frac{U_m}{U_p} = \sqrt{\frac{K_{Tm}}{K_{Tp}}\left(\frac{L_p}{L_m}\right)^3} = 0.78 \tag{12}$$

As shown below, this results in a minimum velocity for the onset of the instability around 8 m/s, which is small enough to accurately measure the phenomenon without applying excessive forces to the model, and large enough to maintain an adequate *Re* number and reduce uncertainty in the measurement of fluid dynamic variables.

In the tests conducted, no significant influence of the shape of then torque tube has been found, nor the variation of the cross section all along the axis.

2.3.3. Natural frequencies

The torsional frequency of the model is f_{Tm} = 20.85 Hz, complying with the frequency relationship between the model and prototype:

$$\frac{f_{Tm}}{f_{Tp}} = \frac{U_m L_p}{U_p L_m} \quad \textbf{(13)}$$

The mass of the panels and purlins can be calculated from the density of the used *PLA* (1240 kg/m3): M_m = 0.0991 kg. This also complies with the similarity relationship:

$$\frac{M_m}{M_p} = \left(\frac{L_m}{L_p}\right)^3 \quad \textbf{(14)}$$

The purlins have been dimensioned to meet the flexural stiffness relationship:

$$\frac{(EI)_m}{(EI)_p} = \left(\frac{U_m}{U_p}\right)^2 \left(\frac{L_m}{L_p}\right)^4 \quad \textbf{(15)}$$

Considering that the Young's modulus of *PLA* is E = 3.50 GPa, the flexural stiffness obtained from the geometry is $(EI)_m$ = 0.17 N·m^2, which is only 1.6% lower than required.

2.3.4. Support pillars

The support pillars have been engineered to hold the torsion tube at a height of 100 mm above the ground, and the cross section is 11 mm x 6 mm to ensure sufficient stiffness. It is notable that the bending frequencies of the columns are an order of magnitude higher than the frequencies considered above. If the pillars were slimmer, this aspect would have to be given greater consideration. A conical grip to reduce friction with the tube and minimize the effects of angular misalignments (Figure 4a) has been designed. The grips are open to facilitate assembly (Figure 4b). According to the selected prototype and scale, there are three pillars. During their placement in the test chamber, it is crucial that they are correctly aligned with the axis. Otherwise, the forces in the supports can substantially increase friction. PLA clamps have been used to attach the pillars to the floor and simplify positioning.

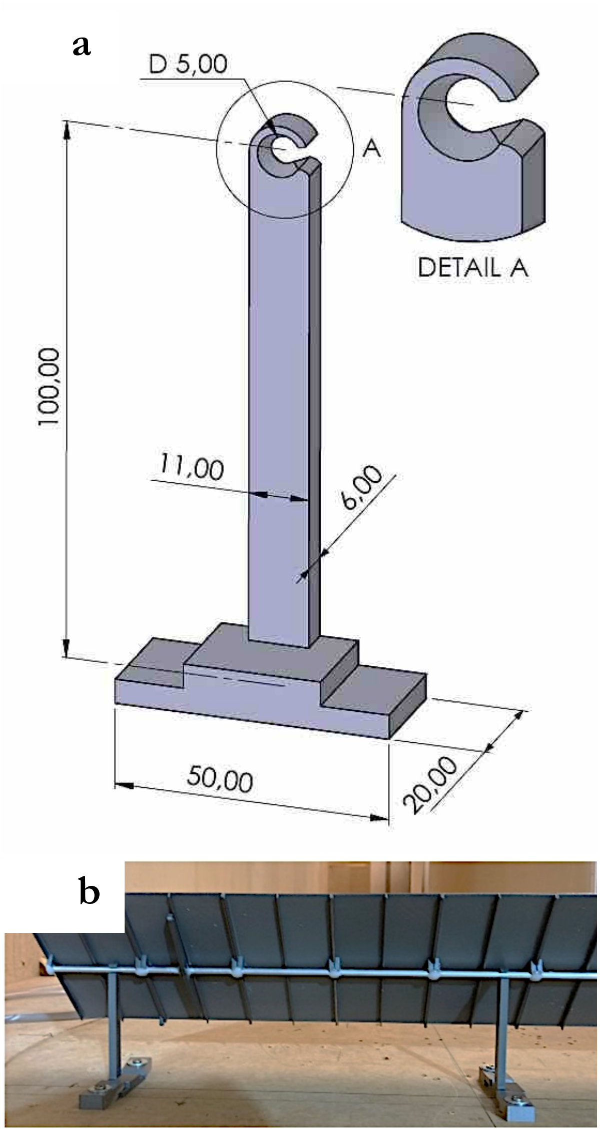

Figure 4. a) technical drawing of the support pillars with a detail of the grip; b) assembling.

2.3.5. Fixed support

At the end of the tracker corresponding to the position of the driver, which is also the plane of symmetry, the torque tube is bound using a cap ending in a cylinder 10 mm wide and 40 mm in diameter. The cap is thick enough to prevent torsion and limit the effective length of the torque tube to 960 mm. The tube is attached to the cap with screws and adhesive. This cap is supported by a thicker pillar ending in a bracket, completely restricting the displacement and rotational movement of the torque tube at that end. This ring closes with a screw that allows to set the tracker tilt (Figure 5).

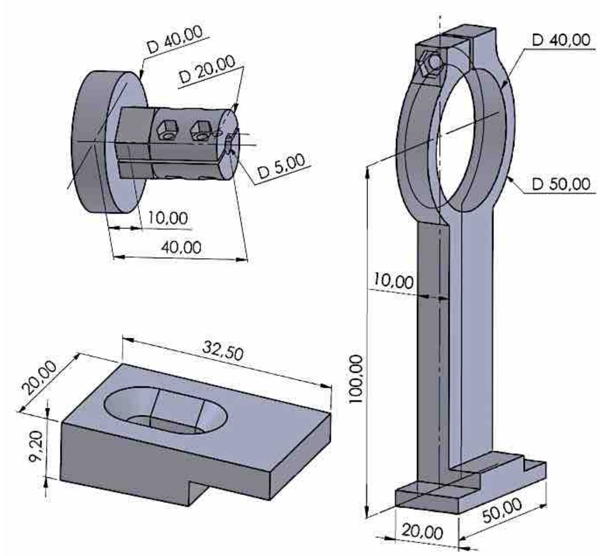

Figure 5. Technical drawing of the cap, clamp and the fixed support.

Table 1 summarizes the geometrical and mechanical specifications for both prototype and scale model:

Tabla 1. Prototype and model characteristics.

	Prototype	Scale model
N panels	48	12
N pillars	1 (driver) + 3	1 (driver) + 3
Panel size	2.40 x 1.20 m	0.160 x 0.080 m
Confg.	2P	2P
L	28.80 m	0.960 m
b	4.80 m	0.160 m
AR	12	12
H	3.00 m	0.100 m
D	0.20 m	0.005 m
e	0.004 m	0.0005 m
h_p	0.24 m	0.008 m
K_T	$6.64{\cdot}10^4$ N·m	1.51 N·m
f_T	0.90 Hz	20.85 Hz
M	2592 kg	0.099 kg
I_R	$5.14{\cdot}10^3$ kg·m^2	$2.17{\cdot}10^{-4}$ kg·m^2
EI	$2.30{\cdot}10^5$ N·m^2	0.17 N·m2

3. Experimental methodology

The objective of the experimental tests conducted on the previously defined tracker model is to obtain precise and replicable information about its aerodynamic behavior, specifically the critical speeds for the onset of the torsional instability. This velocity has been obtained by reducing the speed of the wind tunnel, starting from the state of instability of the scale model. and the tracker's axis perpendicular to the flow. A wide range of angles was tested, with particular attention to angles close to the horizontal.

Typically, the instrumentation used consisted of: Wenglor *CP35MHT80* laser distance sensors to measure the angle variation at the tracker's end (resolution of 50 µm, linearity of 0.15%, accuracy in angle measurement 0.07 degrees); a video system with two Ranger *RC* webcams (resolution of 4K) for continuous monitoring of the test and model movements; an "in house" balance made (Figure 6) of two load cells of 0.78 kg to obtain the torque at the fixed end (accuracy 0.1%, uncertainty 1.8%). Additionally, a digital oscilloscope (*KEYSIGHT EDUX1052A*) was used to analyze the measurements during the test.

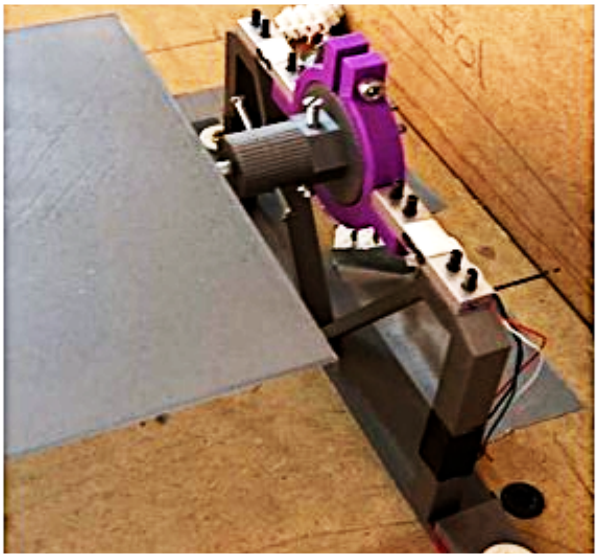

Figure 6. Detail of the force balance.

The data was acquired using an *ADLINK USB-2401 DAQ* module (resolution 24 bits, 4 channels simultaneously, maximum rate of 2 kS/s). The measurements were performed with an acquisition frequency of 2000 Hz, and 76800 data points from each sensor. The data were collected and processed in *Matlab*, using programs specifically developed by the research team. The tests were independently performed in two wind tunnels, one at the University of Oviedo (Figure 7a and 7b) and the other at the Polytechnic University of Madrid (Figure 7c).

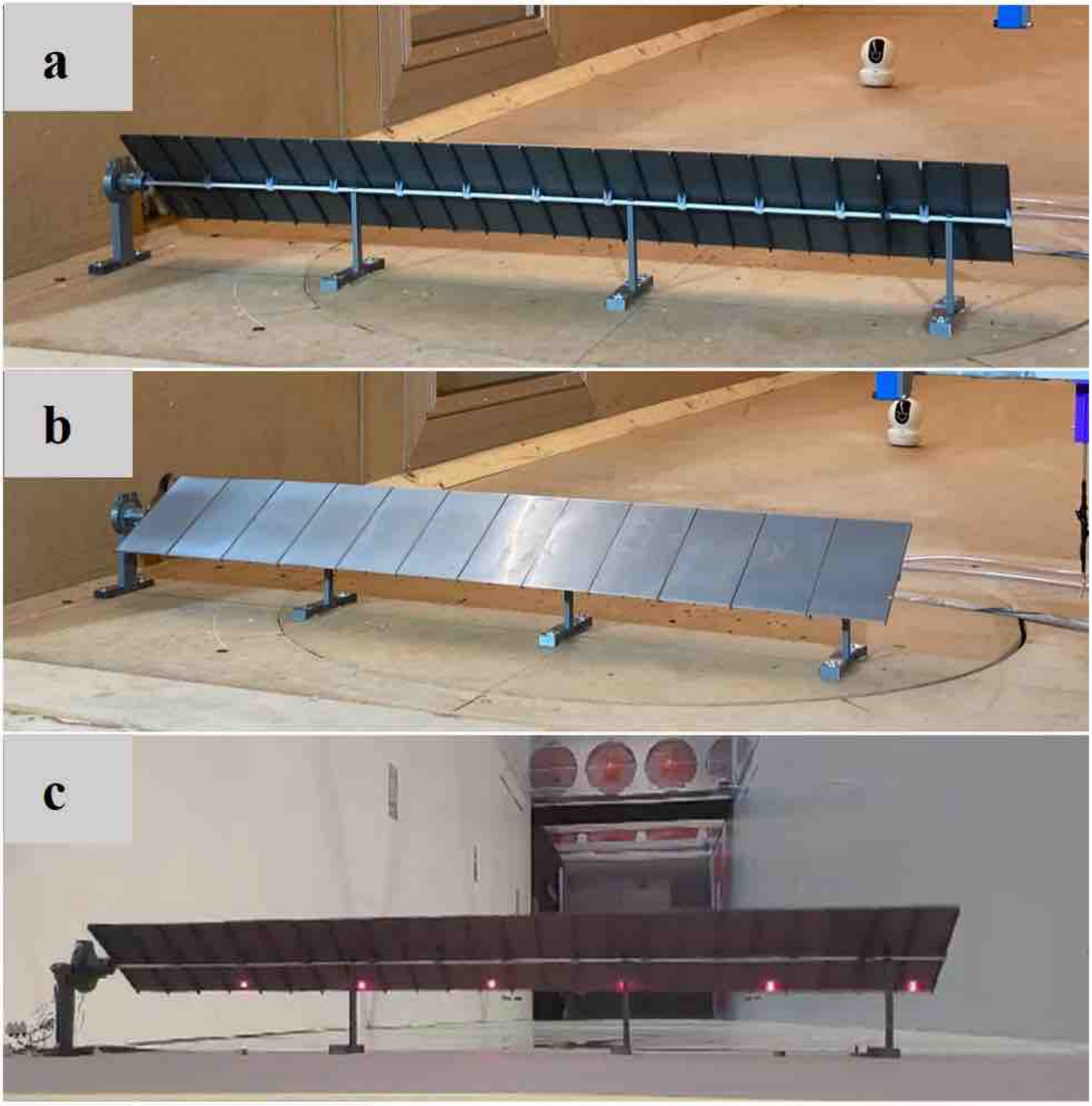

Figure 7. Tracker setup in the test chamber; a-b) University of Oviedo; c) UPM IDR, Madrid.

3.1 Wind tunnel specifications

The wind tunnels have a 1.50 and 2.20 m test chamber, respectively; blockages were below 4% and *Re* ranged from $8.00 \cdot 10^4$ and $1.50 \cdot 10^5$. To guarantee controlled and easily reproducible conditions, the tests were conducted in uniform and low turbulence flow. Figure 8 shows the boundary layers and turbulence non-dimensional power spectrum of the main flow.

3.2 Natural frequency and damping of the scale model

The natural frequencies of the model and the damping were experimentally determined through free vibration tests. The principal natural frequency associated with the torsional mode of the structure is 17.25 Hz. This frequency is slightly lower than the theoretically calculated 20.85 Hz. The reason for this discrepancy is that the torsional stiffness, which depends mainly on the Shear Modulus of the material, is lower than expected. The inertia of the panels has been checked weighting the panels. Although the difference is small, these factors underscore the importance of experimentally measuring the torsional frequency, rather than relying on theoretical calculations. The damping coefficient, ζm = 0.027, aligns quite well with the typical values of metallic structures. Previous research has found that, for natural values of damping (without external damping), this dimensionless number does not influence the critical velocity of the instability.

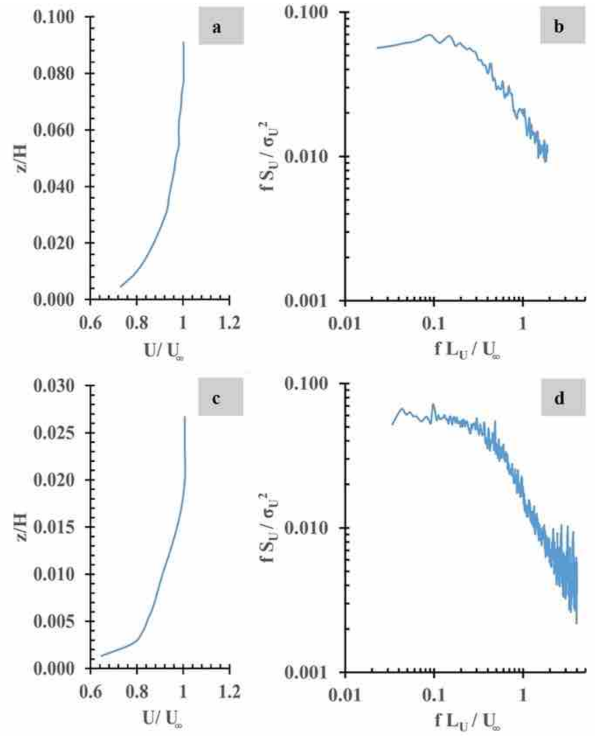

Figure 8. Boundary layers and turbulence; a) and b) ACLA16 at UPM IDR, Madrid; c) and d) ETHAN50-ABLWT at University of Oviedo.

4. Results

One of the main results (among many others) obtained from the proposed benchmark and methodology is the critical velocity for the so-called torsional instability (1 DOF Flutter), which can be seen in Figure 9.

This study has been focused in the determination of the Stability Diagram of the Tracker (Figure 10). The value of 1 degree RMS for, at least, 10 seconds was considered the optimal choice for detecting instability early on, without being affected by signal alterations. With respect to the time, 10 s on the model corresponds to 3.80 minutes in the prototype.

Figure 9. Twisting of the Benchmark model in developed torsional instability.

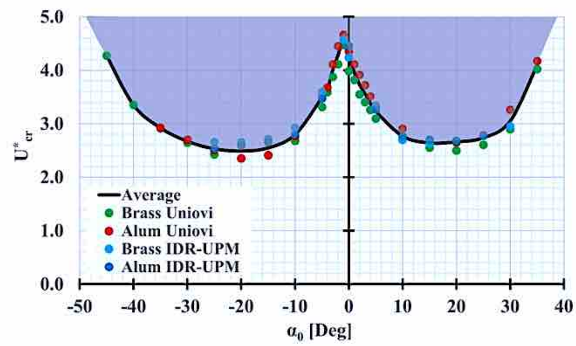

Figure 10. Stability Diagram of the Tracker.

The phenomenon is complex; Figure 11 shows a moke visualization performed by the authors.

Figure 11. Torsional instability visualization.

It exhibits different characteristics for various tilt angles. For tilt angles about 10º to 35º and -10º to -45º it can be said that it is generated by the aeroelastic interaction between the tracker torsion and the vortex at the leeward side of the leading edge. In a simplified way, the vortex oscillation causes the aerodynamic force to fluctuate, thus changing the panel torsion, and the panel torsion generates a larger vortex oscillation. For tilt angles roughly between -10º to 10º there are several explanations, still under thoroughly investigation.

5. Conclusions

In the present study, a reference model of a single-axis photovoltaic solar tracker has been defined, reproducing the basic geometry and structure of typical commercial trackers. An analysis of the similarity conditions associated with the aeroelastic behavior of the trackers has been presented, including the determination of the first natural frequencies for the torsion of the torsion tube (both from structural properties and experiments), the dimensionless coefficients for panel bending and system damping.

The proposed canonical model has been tested in two wind tunnels, one at the Polytechnic University of Madrid and the other at the University of Oviedo, having found a perfect agreement between the results. Therefore, it is expected that this Benchmark will function as a reference point for the homologation of studies on tracker aeroelasticity and will provide reliability to the resulting data, thereby overcoming the current limitations of standards.

Acknowledgements

To ESOLIA & SOLTRACK team, from both Polytechnic School of Madrid ("Instituto de Microgravedad Ignacio da Riva, IDR") and University of Oviedo (Department of Energy, Polytechnic School of Mieres, EPM).

This work is part of the project TED2021-130341B-C21 funded by MCIN / AEl / 10.13039 / 501100011033, the European Union "NextGenerationEU" / PRTRand project PIDZOZ2-1376300B-C21 financed by MCIN / AEl / 10.13039 / 501100011033 / FEDER, UE.

References

[1] C. Rodríguez-Casado, E. Martínez-García, R. Manzanares-Bercial, J.L. Ruiz-Moral, E. Blanco-Marigorta, A. Navarro-Manso, Experimental Benchmark for the 3D wind tunnel testing of torsional aeroelastic instabilities in single-axis solar trackers, Journal of Wind Engineering and Industrial Aerodynamics. 253 (2024), 105838.

[2] S. Franchini, M. Ogueta-Gutiérrez, O. Gómez-Ortega, R. Manzanares Bercial, E. López Núñez, A. Moralejo, Prediction and controlling torsional instabilities in photovoltaic solar trackers, in: The 15th International Conference on Wind Engineering, 2019.

[3] A. Roedel, Extreme weather protection: how to 'weatherise' a solar installation, 2021 www.pv-tech.org 53–57.

[4] A. Roedel, S. Upfill-Brown, Designing for the wind: Using dynamic wind analysis and protective stow strategies to lower solar tracker lifetime costs, Nextracker, 2018.

[5] C. Rohr, P.A. Bourke, D. Banks, Torsional Instability of Single-Axis Solar Tracking Systems, in: 14th International Conference on Wind Engineering, 2015

[6] Z.J. Taylor, M.A. Feero, M.T.L. Browne, Aeroelastic instability mechanisms of single-axis solar trackers, Journal of Wind Engineering and Industrial Aerodynamics. 244 (2024).

[7] A. Ricci, Structural Design of Mono Axial Tracker: Wind Loads and Aerodynamic Design, 2020.

[8] E. Martínez-García, E. Blanco-Marigorta, L. Parrondo Gayo, A. Navarro-Manso, Influence of inertia and aspect ratio on the torsional galloping of single-axis solar trackers, Engineering Structures. 243 (2021).

[9] M.T.L. Browne, Z.J. Taylor, S. Li, S. Gamble, A wind load design method for ground-mounted multi-row solar arrays based on a compilation of wind tunnel experiments, Journal of Wind Engineering and Industrial Aerodynamics. 205 (2020).